# Reinventing Molecular Imaging with Total-Body PET, Part II: Clinical Applications

Babak Saboury, MD, MPH[a,b,c], Michael A. Morris, MD, MS[a,b],
Moozhan Nikpanah, MD[a], Thomas J. Werner, MS[c],
Elizabeth C. Jones, MD, MPH, MBA[a], Abass Alavi, MD[c],*

### KEYWORDS

• Total-body PET • Oncoradiology • Oncology • Inflammation imaging • Vascular imaging

### KEY POINTS

- Total-body PET scans will make immuno-PET imaging and multitracer profiling feasible through delayed imaging and reduced radiation dose.
- As a result, multidimensional evaluation of disease heterogeneity in vivo will be practical in the clinic.
- Total-body PET dynamic whole body imaging allows simultaneous functional and molecular evaluation of multiple organ systems, a concept termed systems biology imaging.
- Total-body PET systems biology imaging allows the further development and clinical implementation of more robust global disease assessment capabilities.

## INTRODUCTION

Total-body PET (TB-PET) imaging is an evolving technology addressing the limitations of conventional PET imaging. With a fundamentally novel approach for its geometric coverage to encompass the entire body, TB-PET imaging has the potential to dramatically increase the effective sensitivity of PET scans. The increased sensitivity could be used for different strategies, such as enhancing the signal-to-noise ratio, improving temporal resolution, or requiring less radioactivity at the time of imaging (**Table 1**).

In Part I of this 2-part article (see Babak Saboury and colleagues' article, "Reinventing Molecular Imaging with Total-Body PET, Part I: Technical Revolution in Evolution," elsewhere in this issue), we provided an overview of the technologic gains of the TB-PET scanner. In this second part, we discuss the practical advantages that this technology can bring about to specific clinical applications of PET imaging (**Fig. 1**).[1,2]

## PRACTICAL CLINICAL APPLICATIONS

Conventional PET imaging techniques have been shown to suffer from significant limitations in clinical use to assess disorders that are diffuse in nature and involve many structures throughout the body. The major shortcomings are due to the limited sensitivity and limited field of view of approximately 20 to 30 cm, which requires imaging the entire body in a fractionated manner over an hour or longer to determine the extent of the disease at its various stages.[3] However, based on the experience that has been gained over the years, most disease abnormalities are best assessed by imaging the entire body to detect

---

**Table 1**
**Improved sensitivity of the TB-PET scanner can result in better signal-to-noise ratio (SNR), enhanced temporal resolution (T), or reduction of the required dose of the radiotracer (A)**

**Eq. 1**

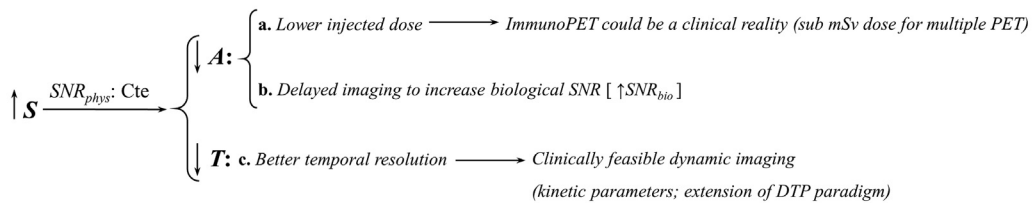$$SNR_{phys} \approx k\sqrt{S \times A \times T}$$

$SNR_{phys}$: *Signal-to-Noise Ratio (physical system)*

$S$: *Effective Sensitivity*

$A$: *Radioactivity at the time of imaging*

$T$: *Imaging time*

**Eq. 2**

$\uparrow S \xrightarrow{SNR_{phys}: Cte}$

$\downarrow A$:
a. *Lower injected dose* ⟶ *ImmunoPET could be a clinical reality (sub mSv dose for multiple PET)*
b. *Delayed imaging to increase biological SNR* [ $\uparrow SNR_{bio}$ ]

$\downarrow T$: c. *Better temporal resolution* ⟶ *Clinically feasible dynamic imaging*
*(kinetic parameters; extension of DTP paradigm)*

---

unexpected lesions that may or may not be related to the primary sites. This is particularly applicable to the adult population, who are prone to developing many age-related maladies. Among these, we would like to emphasize the role of TB-PET imaging in examining patients with cancer, inflammatory and immunologic disorders, cardiovascular disease, and osteoporosis, which are known to involve many structures and organs in the body.

## Global Disease Assessment and Systems Biology

The concept of a global disease assessment (GDA),[4] with the aim of quantifying the total burden of disease by combination of structural and molecular information, has gained popularity in recent years.[5–7] GDA is a method whereby a single or composite quantitative value, the Global Disease Score,[8] represents the burden of an ongoing disease process over the course of disease beginning at a baseline point and compared throughout subsequent therapeutic interventions (**Figs. 2** and **3**).[9,10] Hybrid molecular and structural imaging with PET and computed tomography (CT) scans or MR imaging as a single imaging instrument seems to be the approach of choice for such novel applications. GDA methodology has been adopted for assessing regional and global disease activity in many disorders, particularly those that are systemic in nature. Novel approaches have been described in the literature that demonstrate this technique's unique ability to quantify the degree of abnormality in various organs and throughout the body. Data from the approach have similarly demonstrated great importance in patients with cancer, atherosclerosis, systemic inflammation, and musculoskeletal disorders.[11–18]

TB-PET imaging will be of unique importance in improving temporal resolution to better reflect overall disease burden and will allow for better management of many serious, disabling, and potentially fatal diseases and disorders. TB-PET imaging has the potential to expand the concept of dual time point–derived GDA by extracting the kinetic parameters. Both dynamic whole body imaging and the ability to perform more delayed imaging provide a mechanism to study whole body pathobiology kinetics.[8] GDA-based biological systems state quantification and systems interrelation characterization through time is the basis for a systems biology approach to medical imaging.

In clinical practice, TB-PET could be used for faster performance, a decreased patient dose, and enhanced capacity to make delayed imaging and dynamic whole body imaging possible. These technical capabilities lead to a unique usefulness: making systems biology imaging a reality. The human body is a complex, dynamic system with inherent interconnectedness; the boundaries between organs and systems have faded by new advancements in our understanding of the pathologic basis of disorders. The significant role of the immune system in disease makes this
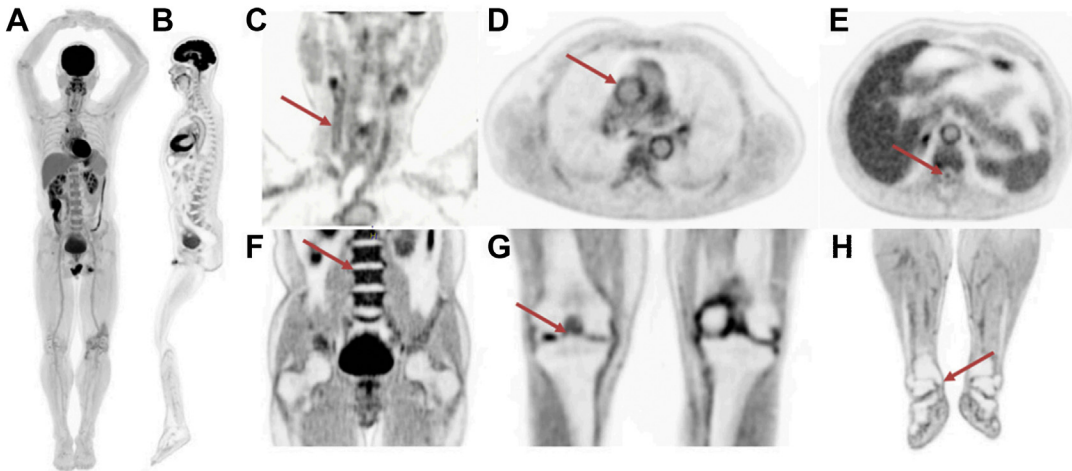
**Fig. 1.** Total-body PET scan of a patient who was injected with 290 MBq of $^{18}$F-FDG. A 20-minute list-mode scan was performed at 82 minutes after injection on the EXPLORER scanner. (*A*) Total-body maximum intensity projection (MIP). (*B*) Total-body sagittal view that was generated from the 20-minute scan. Selected views including (*C*) head and neck view, showing walls of the right carotid artery (*arrow*). (*D*) Chest view, demonstrating walls of ascending aorta (*arrow*), (*E*) midthoracic view, showing spinal canal (*arrow*), (*F*) abdominal and pelvic view, indicating clear delineation of the superior endplate of L3 (*arrow*), (*G*) knees, showing bone spur on the right side (*arrow*), and (*H*) lower extremities, indicating defined medial tibial malleolus of the right side (*arrow*). (Originally published in Badawi RD et al. First Human Imaging Studies with the EXPLORER Total-Body PET Scanner. J Nucl Med 2019;60:299-303. © SNMMI.)
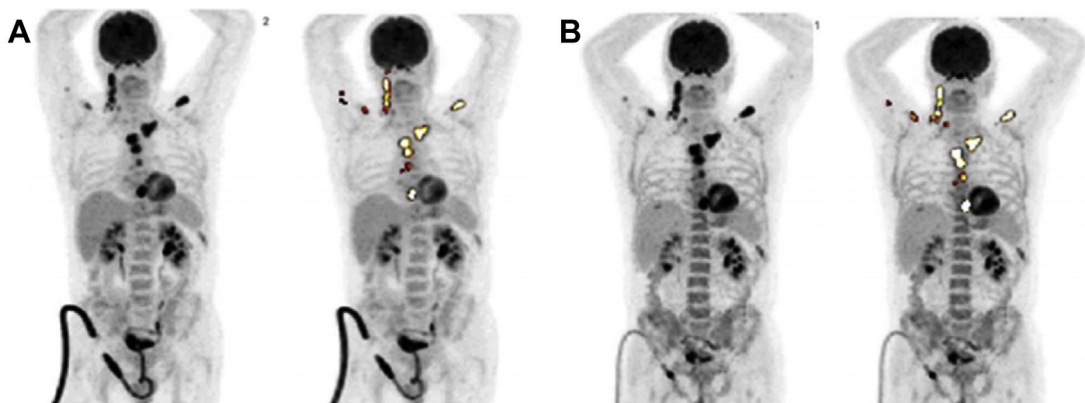


|  | 60 min | 180 min | Percentage of change |
|---|---|---|---|
| SUVmean (CR Lesions) | 5.95 | 7.29 | 22.52% |
| SUVmean (PR Lesions) | 5.58 | 6.98 | 25.08% |
| pvcSUVmean (CR lesions) | 9.04 | 11.28 | 24.77% |
| pvcSUVmean (PR lesions) | 8.55 | 11.42 | 33.56% |

**Fig. 2.** Maximum intensity projection (MIP) FDG PET/CT scans of a 60-year-old patient with multiple myeloma (*A*) pretreatment 1 hour and (*B*) pretreatment 3 hours after administration of FDG. Table shows the percentage change of mean standardized uptake value (SUV$_{mean}$) and partial volume correction (pvc) of the SUV$_{mean}$ of the complete response (CR) and partial response (PR) lesions from 1-hour to 3-hour scans. (Originally published in Raynor, William Y., Abdullah Al-Zaghal, Mahdi Zirakchian Zadeh, Siavash Mehdizadeh Seraj, and Abass Alavi. 2019. "Metastatic Seeding Attacks Bone Marrow, Not Bone: Rectifying Ongoing Misconceptions." PET Clinics 14 (1): 135–44.)
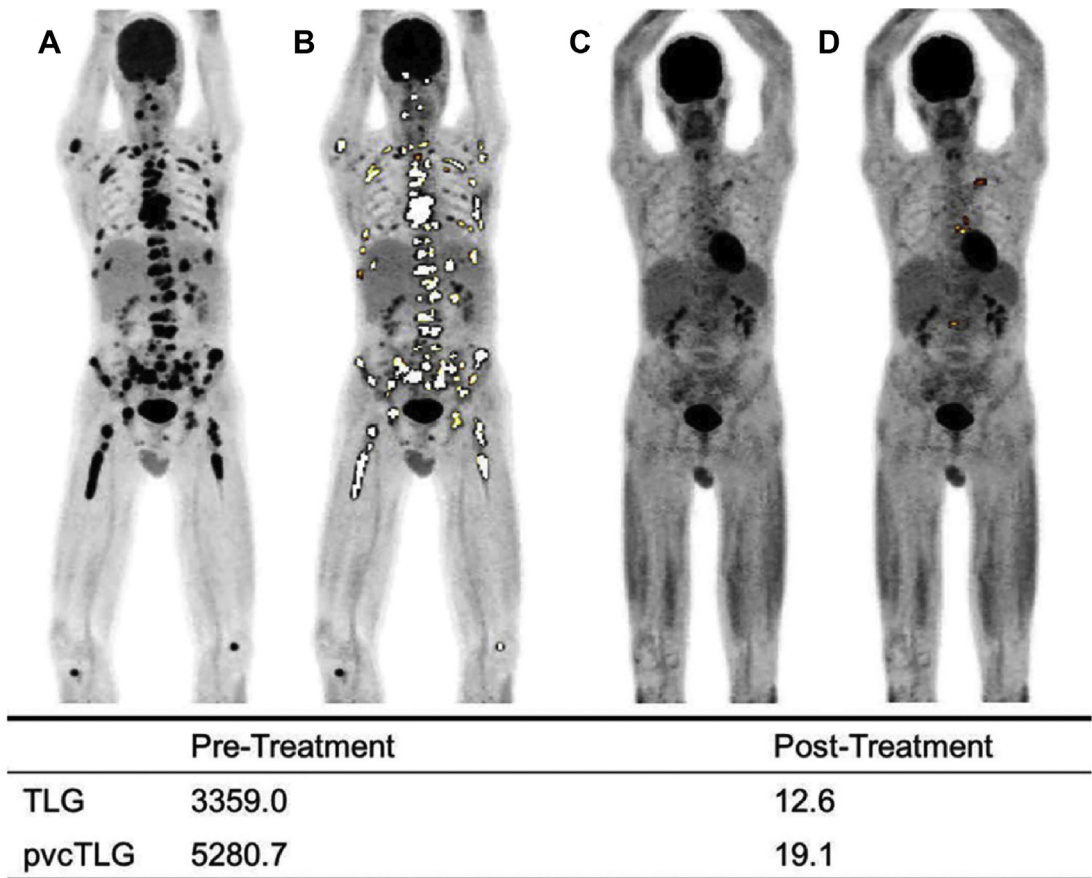
**Fig. 3.** FDG PET examinations in a patient with multiple myeloma showing maximum intensity projection (MIP) images at baseline (*A*) with GDA applied (*B*), and on follow-up 2 months after high-dose chemotherapy (*C*) with GDA applied (*D*). Adaptive thresholding algorithm was used (ROVER software; ABX GmbH). (Originally published in Raynor, W.Y., Zadeh, M.Z., Kothekar, E., Yellanki, D.P. and Alavi, A., 2019. Evolving Role of PET-Based Novel Quantitative Techniques in the Management of Hematological Malignancies. PET clinics, 14(3), pp.331-340.)

interconnectedness much more explainable. Cardiovascular manifestations of the autoimmune disorders are only the tip of the iceberg.[19,20]

In complex systems theory, a system is composed of multiple interconnected subsystems. Subsystems are characterized by their state at each given time. The relation between subsystems only depends on their respective state and subsystems are not exposed to another's inner complexity. GDA thereby reflects the state of each system. This decrease in complexity is an essential prerequisite of building the system of subsystems, providing a framework to expand our understanding of the whole. The study of the interrelation of subsystem states at 1 time (synchronous) and through time (metachronous) was limited by the spatial and temporal constraints of conventional PET imaging. TB-PET imaging is a tool for systems biology par excellence.[21,22]

## Oncology

### Dose reduction

The increased sensitivity of TB-PET imaging can be used to decrease the required amount of activity at the time of imaging. This property will significantly contribute to decreasing the radiation dose delivered to patients. This capability opens the door for 3 particular use cases: multitracer PET imaging, shorter follow-up PET imaging, as well as immuno-PET imaging (see **Table 1**, Equation 2a).

1. By now, it is clear that cancer is a heterogeneous disease by nature and that tumor heterogeneity is the hallmark of treatment failure.[23] Using multiple tracers for imaging the tumor biology has a potential advantage.[24] Previously, the exposure dose was one of the drawbacks preventing this type of PET imaging. Some researchers alluded to this potential possible in routine standard of

care, such as the benefits of synergistic PET imaging for prognostication, as demonstrated by fludeoxyglucose (FDG) and HER2 PET in the ZEPHIR trial (**Fig. 4**).[25,26]

2. Treatment response follow-up by molecular imaging has shown value for personalized patient management, yet the exposure dose has also played a negative role in the expansion of this paradigm.

3. It is almost impossible to justify the radiation exposure of immuno-PET imaging in daily clinical practice outside of research studies. Attempting to characterize tumor heterogeneity with multiple immuno-PET tracers in series with conventional PET imaging could expose the patients to more than 100 mSv on conventional PET imaging. This factor could dramatically change in the TB-PET imaging era.

### Delayed imaging

In addition to radiation dose reduction, the need for a lesser amount of radiotracer in TB-PET imaging provides opportunities for delayed imaging where the sensitivity of the scanner for detecting the metabolic activity is of utmost importance (see **Table 1**, Equation 2b). As described in Part I of this 2-part article (see Babak Saboury and colleagues' article, "Reinventing Molecular Imaging with Total-Body PET, Part I: Technical Revolution in Evolution," elsewhere in this issue), delayed imaging can improve the biological signal-to-noise ratio. Based on numerous research studies that have been conducted during the past 2 decades, it has become apparent that the degree of uptake of FDG in malignant tissues increases over time and reaches a plateau at around 4 to 5 hours after administration of the compound.[27–29] Basu and colleagues[29] showed a continuous increase in FDG uptake of the lung cancer lesions up to 8 hours after injection. This phenomenon not only allows detecting the presence of cancer activity at the primary sites, but also improves the sensitivity of the technique for accurately staging the disease by visualizing metastases to the lymph nodes and different organs in the body. In addition, our group demonstrated FDG uptake decreases significantly from 1 to 3 hours after injection in the majority of normal tissues, except heart and bone marrow.[30] This property further enhances the contrast between tumor site activity and the surrounding background.[30] However, the bone marrow retention of FDG could be detrimental in detection of bone marrow metastatic lesions in delayed imaging, and this drawback should be considered in study designs. Overall, delayed imaging enhances the impact of FDG-PET imaging in the management of patients with various malignancies at various stages of the disease. Using the principles that our group previously described, some of the researchers speculated that TB-PET imaging could improve detection of micrometastases, which are smaller than 5 mm.[31]

### Dynamic imaging

The combination of full field of view and enhanced temporal resolution in TB-PET imaging would allow improved dynamic quantification of radiotracer uptake over time (see **Table 1**, Equation 2c). The extraction of kinetic analysis parameters has already been clearly proven in the realm of FDG PET imaging. Our group extensively demonstrated the value of multiple time-point imaging in
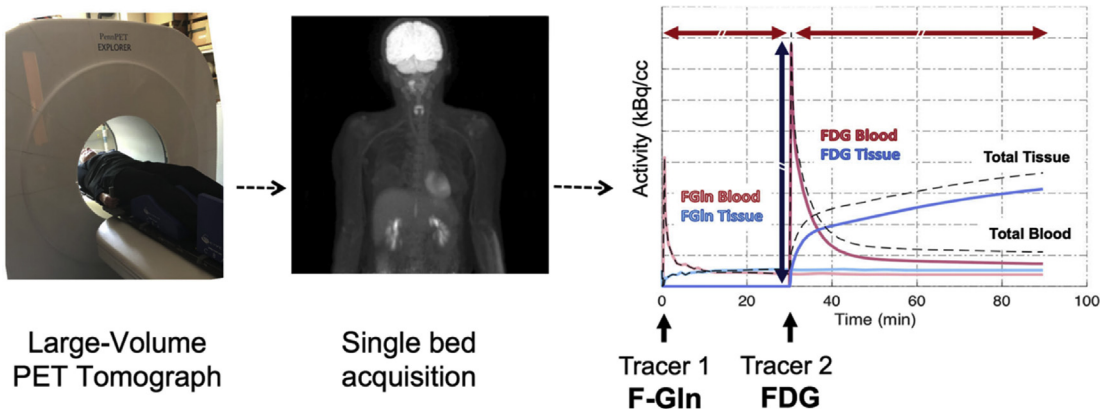


**Fig. 4.** Time–activity curves in a patient imaged in the prototype PennPET Explorer using low-dose $^{18}$F-FGln first (*left*), followed by higher dose $^{18}$F-FDG (*right*) for dual tracer PET imaging in series to model both glutamine and glucose metabolism in a single bed position, in a single encounter. (Originally published in Mankoff, David A., Austin R. Pantel, Varsha Viswanath, and Joel S. Karp. 2019. "Advances in PET Diagnostics for Guiding Targeted Cancer Therapy and Studying In Vivo Cancer Biology." Current Pathobiology Reports 7 (3): 97–108.)

tumor biology characterization.[28,32,33] Tumors with an increasing standardized uptake value over time are suggested to be more aggressive than those with a decreasing standardized uptake value over time.[34] There is limited literature available on the investigation of dynamic changes in other radiotracers within a single patient encounter, which is an area of important future investigation.

### Systems Biology Approach to Cancer Imaging

As patients begin to live longer with chronic malignancies, dynamic imaging with TB-PET scans will also help to manage multisystemic effects of oncologic processes as well as side effects of treatments on body organs and systems (cancer as a chronic disease paradigm). A similar paradigm can be exemplified in the changing approach to patients with human immunodeficiency virus infection as more effective treatments became available.

### Atherosclerosis

Patients with malignancies have a high incidence of atherosclerosis.[35–37] Currently, this serious complication is a major domain of research and interest in the population with cancer, particularly in patients with prostate cancer, hematologic malignancies, and some others whose disease can be controlled for an extended period of time. Clearly, the high incidence of atherosclerosis in these patients may lead to significant morbidity and mortality that are unrelated to their underlying disorders.[38,39] Both FDG[40] and $^{18}$F-sodium fluoride (NaF),[41–43] which are commonly used for PET imaging of patients with various malignancies, are optimally suited for detecting atherosclerotic plaques in the arterial system throughout the body. Again, delayed imaging with total-body machines allows significant clearance of these tracers

from the circulation and therefore optimal visualization of atherosclerotic plaques. As such, total-body imaging at delayed time points may improve the ability to detect and treat vascular complications of various cancers with higher sensitivity and specificity.[44]

### Venous thrombosis

It is well-established that the second most common cause of death among patients with cancer is pulmonary embolism. Most malignancies (with a higher incidence in certain cancers) are associated with a high incidence of clot formation in the venous system throughout the body. Research and clinical studies have shown high uptake of FDG in active clots throughout the body (**Fig. 5**).[45–47] This is due to the presence of activated white cells and platelets in actively forming clots. Therefore, FDG-PET imaging for assessing patients with cancer will allow detecting the presence of clots throughout the body, including in the lower extremities (**Fig. 6**). As such, by adopting the limited body imaging protocols, many instances of venous thrombosis in the lower extremities are frequently missed. Therefore, total-body imaging by dedicated TB-PET systems will play a major role in the early detection and treatment of venous thromboembolism in patients with malignant disorders.

### Hyperinflammatory state

The process of oncogenesis is not merely invasion of tumor cells throughout the body. There is extensive interaction between the immune system and tumor cells, which results in significant control of the disease. This paradigm of healing from within resulted in novel treatment options, from immune-check-point inhibitors to chimeric antigen receptor T-cell therapy.[48,49] Engagement of the immune system in this prolonged battle on the one hand and effects of treatment options, on
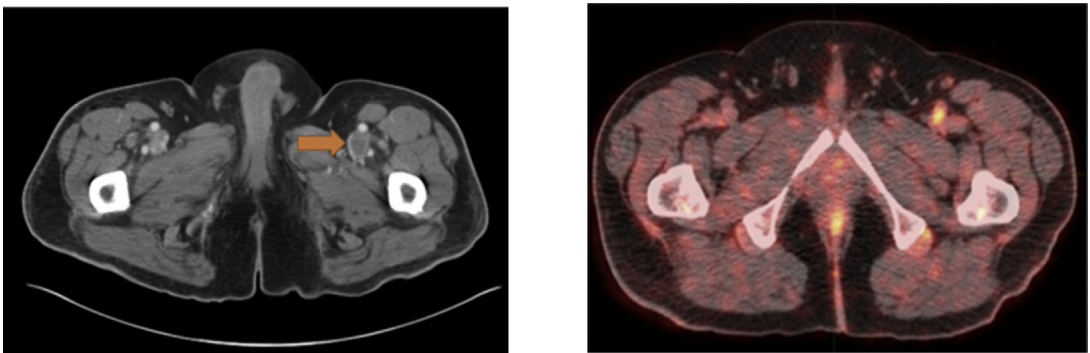


**Fig. 5.** Patient with a history of new non-occlusive thrombus involving the left renal vein with concern for deep vein thrombosis involving the left common femoral vein. (*left*) Axial contrast-enhanced CT scan, and (*right*) axial fused $^{18}$F-FDG PET/CT scan showing increased FDG uptake within the filling defect within the left common femoral vein (*arrow*) suspected to correspond with deep vein thrombosis in this location.
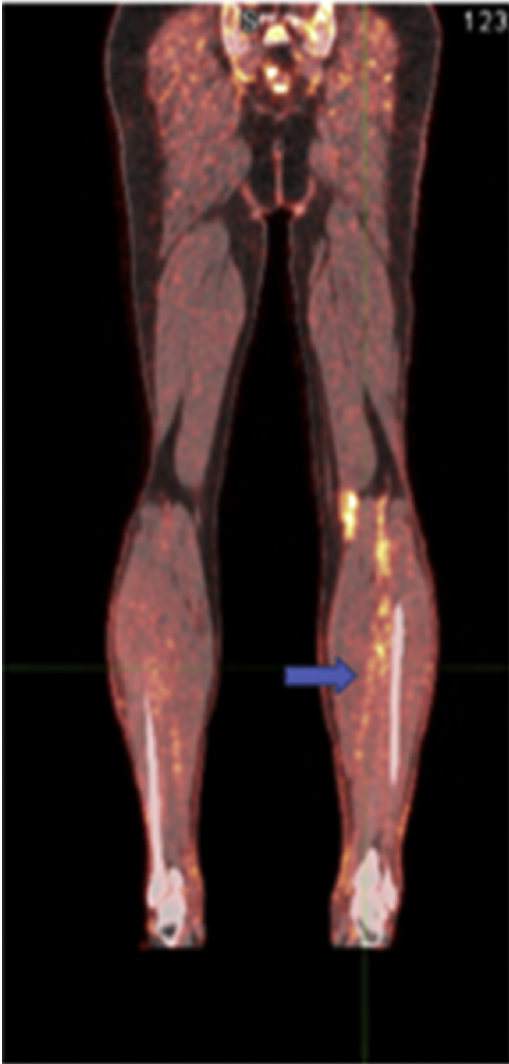
**Fig. 6.** A 65-year-old man with melanoma on the left upper back, on BRAF/MEK inhibitor since April 2012, which was held on December 21, 2012, secondary to toxicity, with biopsy-proven gastric metastasis and left axillary nodal metastasis. One day before the PET scan, the patient had 2+ edema from the mid-upper arm to the hand and 1+ edema in the left calf and foot. A coronal fused $^{18}$F-FDG PET/CT image shows increased metabolic activity within the left lower leg veins (*arrow*) corresponding with an acute deep vein thrombosis.

the other hand, create dysregulation of immune system function, which may result in a subclinical inflammatory state in many organ systems.[48–50] This condition could have long-term negative effects and monitoring this condition could provide invaluable insight in the preventive aspects of chronic cancer care. Although FDG-PET plays a major role in this process, it has certain limitations where the adjacent biological process is also hypermetabolically active. To overcome this limitation, one approach is to use positron-emitting nanoparticles to image macrophages.[51]

### Bone metabolism

Cancer-induced bone loss, through either cytokine dysregulation caused by oncogenesis or calcium metabolism alteration caused by treatment, is a well-established phenomenon. Bone fragility and resulting fractures play an important role in mortality and morbidity of oncology patients. NaF-PET imaging provides invaluable information regarding bone turnover[52] and various quantitative methods have been investigated.[53,54] Evaluation of bone turnover in each patient's follow-up imaging examinations could prevent many devastating disease-related fractures.
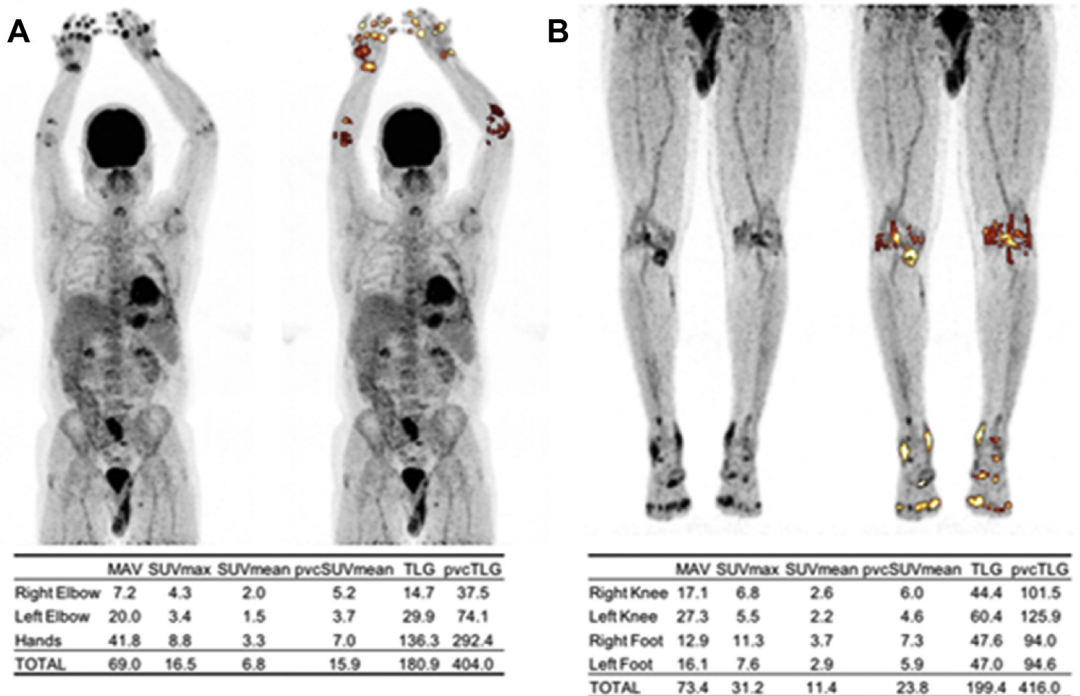
### Metastasis beyond eyes-to-thighs field of view

Although the claim of distal extremity bone marrow metastasis has been mentioned as the grounds for extending the PET field of view beyond conventional base-of-skull to mid-thigh, there is sparse red marrow below the knee in the adult population and the chance of having bone marrow metastasis in such a milieu is extremely rare. Until strong experimental evidence shows contrary, this possibility cannot be a justifying reason for extension of the field of view. However, in pediatric imaging, the presence of red marrow in distal extremities significantly increases such a possibility and mandates head-to-toe imaging.

### Inflammation

Autoimmune disorders are multisystemic by definition,[55] even though the primary manifestation could be in one organ-system. For example, rheumatoid arthritis involves many other systems beyond synovium and joints. Even the joint involvement is not limited to 1 location or even the appendicular skeleton. The patient with rheumatoid arthritis may present with joint problems, but may also develop interstitial lung disease, or C1 to C2 subluxation. Any attempt to quantify rheumatoid arthritis burden of disease by local imaging, such as hand radiographs, is prone to fundamental problems. The lack of a comprehensive imaging biomarker to capture the totality of this disease is a major pitfall in treatment monitoring (hand radiographs are not sufficient). As such, we believe assessing inflammation in various organs and structures as well as osseous abnormalities that are associated with musculoskeletal diseases and disorders will benefit significantly from total-body imaging with PET. Although FDG will be of great value for assessing inflammation and muscle metabolism (**Fig. 7**),

| | MAV | SUVmax | SUVmean | pvcSUVmean | TLG | pvcTLG |
|---|---|---|---|---|---|---|
| Right Elbow | 7.2 | 4.3 | 2.0 | 5.2 | 14.7 | 37.5 |
| Left Elbow | 20.0 | 3.4 | 1.5 | 3.7 | 29.9 | 74.1 |
| Hands | 41.8 | 8.8 | 3.3 | 7.0 | 136.3 | 292.4 |
| TOTAL | 69.0 | 16.5 | 6.8 | 15.9 | 180.9 | 404.0 |

| | MAV | SUVmax | SUVmean | pvcSUVmean | TLG | pvcTLG |
|---|---|---|---|---|---|---|
| Right Knee | 17.1 | 6.8 | 2.6 | 6.0 | 44.4 | 101.5 |
| Left Knee | 27.3 | 5.5 | 2.2 | 4.6 | 60.4 | 125.9 |
| Right Foot | 12.9 | 11.3 | 3.7 | 7.3 | 47.6 | 94.0 |
| Left Foot | 16.1 | 7.6 | 2.9 | 5.9 | 47.0 | 94.6 |
| TOTAL | 73.4 | 31.2 | 11.4 | 23.8 | 199.4 | 416.0 |

**Fig. 7.** FDG-PET maximum intensity projection (MIP) of the upper body (*A*) and lower body (*B*) of a patient with rheumatoid arthritis. Synovial inflammation was assessed by segmenting FDG-avid joints using an adaptive thresholding algorithm (ROVER software, ABX GmbH, Radeberg, Germany). Metabolically active volume (MAV), max standardized uptake value ($SUV_{max}$), mean SUV ($SUV_{mean}$), partial volume-corrected $SUV_{mean}$ ($pvcSUV_{mean}$), total lesion glycolysis (TLG), and partial volume-corrected TLG (pvcTLG) were calculated and summed for each segmented region. The overall pvcTLG for this patient was 820.0.
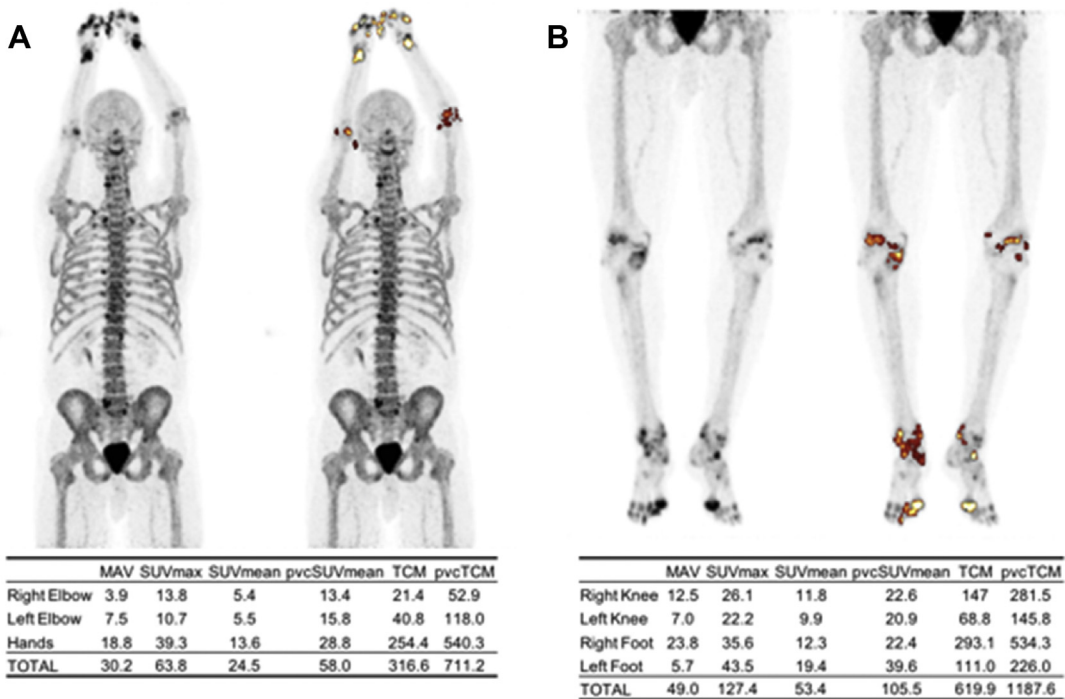
NaF will allow the detection of osseous abnormalities and calcium aberrancies in patients with systemic inflammation (**Fig. 8**). Improved temporal resolution with a 1-minute or less acquisition time is also an advantage that will lead to decreased motion artifact and partial volume effects. This property could be particularly helpful for evaluation of inflammatory diseases of the bowel.[1,56,57] Inflammatory vasculitides often affect multiple body regions.[44]

In addition to autoimmune disorders, viral infections have proven over and over again to be a multisystem disease. The emerging evidence by studying severe acute respiratory syndrome coronavirus-2 pathogenesis (coronavirus disease-2019 disease) is a salient example to remind us that viruses have systemic effects on the body beyond the primary site of infection that may initially go unrecognized.[58,59] Similarly, total-body human immunodeficiency virus burden in vivo has been suggested using TB-PET imaging.[60]

## Cardiovascular

Atherosclerosis, as the most common cause of morbidity and mortality in the elderly population, is a systemic disease and frequently involves many arteries throughout the body.[61,62] Although cardiac and cerebral complications of atherosclerosis are the main causes of morbidity and mortality in the affected population, no other organ is immune to the serious consequences of this disease. Therefore, there is a dire need for an imaging modality that allows screening the entire body for detecting and characterizing atherosclerotic plaques in their early stages and before they cause significant and irreversible damage to various organs in the body. During the past 5 decades structural imaging techniques such as CT, MR imaging, and ultrasound imaging have been extensively used for detection of this disease but they are known to suffer from many shortcomings.[63–65] It is well-established that these modalities are insensitive for the early detection of the plaques and assessing their response to medical and other interventions. During the past 2 decades, attempts have been made to detect and quantify this common disease at the molecular and cellular levels and before it causes structural changes in the arterial system.[66] In particular, PET/CT scans and PET/MR scans have been used to visualize and quantify inflammation and calcification in plaques

**A**

| | MAV | SUVmax | SUVmean | pvcSUVmean | TCM | pvcTCM |
|---|---|---|---|---|---|---|
| Right Elbow | 3.9 | 13.8 | 5.4 | 13.4 | 21.4 | 52.9 |
| Left Elbow | 7.5 | 10.7 | 5.5 | 15.8 | 40.8 | 118.0 |
| Hands | 18.8 | 39.3 | 13.6 | 28.8 | 254.4 | 540.3 |
| TOTAL | 30.2 | 63.8 | 24.5 | 58.0 | 316.6 | 711.2 |

**B**

| | MAV | SUVmax | SUVmean | pvcSUVmean | TCM | pvcTCM |
|---|---|---|---|---|---|---|
| Right Knee | 12.5 | 26.1 | 11.8 | 22.6 | 147 | 281.5 |
| Left Knee | 7.0 | 22.2 | 9.9 | 20.9 | 68.8 | 145.8 |
| Right Foot | 23.8 | 35.6 | 12.3 | 22.4 | 293.1 | 534.3 |
| Left Foot | 5.7 | 43.5 | 19.4 | 39.6 | 111.0 | 226.0 |
| TOTAL | 49.0 | 127.4 | 53.4 | 105.5 | 619.9 | 1187.6 |

**Fig. 8.** NaF-PET maximum intensity projection (MIP) of the upper body (*A*) and lower body (*B*) of a patient with rheumatoid arthritis. Focal areas of high bone formation in the joints were segmented using an adaptive thresholding algorithm (ROVER software, ABX GmbH, Radeberg, Germany). Metabolically active volume (MAV), maximum standardized uptake value ($SUV_{max}$), mean SUV ($SUV_{mean}$), partial volume-corrected $SUV_{mean}$ ($pvcSUV_{mean}$), total calcium metabolism (TCM), and partial volume-corrected TCM (pvcTCM) were calculated and summed for each segmented region. The overall pvcTCM for this patient was 1898.8.

throughout the body.[67,68] FDG-PET imaging has been successfully used to detect inflammation in various organs owing to a variety of causes. Activated inflammatory cells, such as those within atherosclerotic plaques, are highly glycolytic and as such are readily visualized by FDG-PET. Similarly, molecular calcification can be assessed by radioactive fluoride (NaF) in various arteries far in advance of macroscopic calcification that is visualized by CT imaging.[69] By now, the NaF-PET technique has been shown to be very sensitive for detecting early evidence for atherosclerosis in the arterial system throughout the body.[43] As noted elsewhere in this article, delayed imaging (hours after the administration of either FDG or NaF) is essential to achieve successful results.[70–72]

TB-PET imaging instruments are well-suited for assessing patients with atherosclerosis at various stages of the disease. This imaging methodology allows early detection of many diseases and disorders, as well as also careful monitoring of disease course after various interventions. Novel quantitative techniques that have been developed in recent years allow measurement of GDA and provide a single number for disease affecting each organ as well as the entire body. This measurement has been termed the athero burden, when the approach is adopted in patients with suspected or proven atherosclerosis. We believe systematic quantification will be of great value for the management of affected patients.

## Osteoporosis

Osteoporosis is a major source of morbidity and mortality in the elderly population, particularly in postmenopausal women. Osteoporosis can also manifest in patients with cancer as osteoblasts are exposed to chemotherapeutic agents. This metabolic disorder commonly manifests pathologically in the spine and the lower extremities and is associated with significant fractures and complications related to immobility such as pulmonary embolism and high mortality. NaF-PET imaging is increasingly used for early detection of osteoporosis far in advance of its detectability by structural imaging techniques such as dual energy x-ray absorptiometry scans (**Fig. 9**). It is apparent that the diffuse nature of this disorder requires total-body metabolic assessment with a modality that can
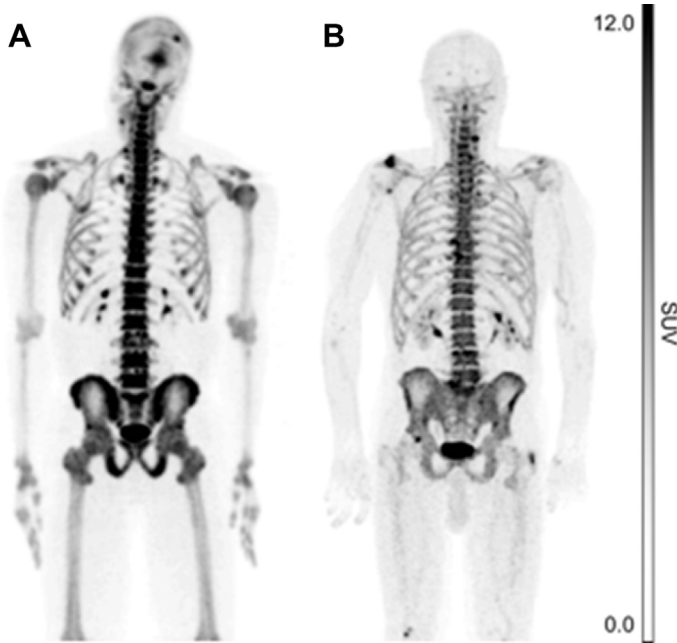
**Fig. 9.** NaF-PET maximum intensity projections (MIP) portraying active calcification in a 36-year-old man (*A*) and a 76-year-old man (*B*). Systemic osteoblastic metabolism was assessed by measuring NaF uptake at the femoral neck and in the whole skeleton. The mean standardized uptake value ($SUV_{mean}$) in the femoral neck and whole skeleton of the younger subject was 6.7 and 5.2, respectively, whereas the $SUV_{mean}$ in the femoral neck and whole skeleton of the older subject was 1.8 and 2.4, respectively.

readily screen for this serious disease. It is possible that TB-PET scanning with NaF will become the modality of choice for both early detection of osteoporosis by innovative global assessment techniques and for the early assessment of response in this population.

Metabolic bone disease could be characterized by NaF TB-PET imaging with sub-mSv patient exposures. Whole body bone metabolism and mineral content could be quantified synergistically by combining TB-PET imaging with photon-counting CT scans.

### Other Applications

In pediatric imaging, TB-PET can make the entire body image acquisition extremely fast[73] compared with the conventional PET-CT instruments with a limited field of view. Longer scans require appropriate measures to decrease the movement of the patient, such as sedation. The need for sedation has deprived pediatric patients of the benefits of many useful imaging techniques. TB-PET imaging can change this challenging situation. In addition to a shorter study time, this technology could significantly decrease the radiation dose. In modern oncology practice, 84% of pediatric patients live for more than 5 years after their diagnosis compared with 58% in the 1970s,[74] and we should be cognizant of the realities of radiation exposure over the long term in these patients.

## SUMMARY

TB-PET provides clinicians the ability to take a comprehensive approach to medical imaging and for imaging scientists may use a systems biology approach to analyze the TB PET images and data. The entire tracer physiology within the patient's body over a given scan time interval can be portrayed, telling a more complete story of the patient's disease process. This information was always present in PET imaging; however, we were limited in our ability to listen. After the injection of a radiotracer to the patient, the patient has paid a fixed cost of radiation exposure. It is our ethical and professional obligation as physicians to obtain as much information as possible for asking the patient to expose himself or herself to that cost. Decreased scan times, lower tracer dose, economies of scale, and added clinical usefulness will also contribute to the economics of TB-PET imaging, which is projected to be a 5- to 6-fold capital investment over conventional PET/CT scans or in the neighborhood of $10 million.[1]

Conventional PET imaging has less signal and therefore less bandwidth compared with TB-PET imaging, as if taking the medical history of a patient, but only listening to 1 word in each sentence. TB-PET imaging allows molecular imaging physicians to sharpen their ears as they listen to the patient, as Osler famously said, "listen to your patient, he is telling you the diagnosis."[75]

Molecular imaging physicians can be more attentive to the patient and his or her disease process through the lens of TB-PET imaging.

Enhanced reimbursement from the TB PET needs to be justified by evidence based studies of the benefits of the TB PET over conventional PET. Various new types of PET examinations made possible by TB-PET imaging need reimbursed commensurate with their clinical value. These new examinations may even be able to occur during the same clinical encounter (performed on the same day, but requiring additional scanner resources and time) or ordered retrospectively after the original data has been acquired (similar to adding an additional laboratory test to a previously acquired phlebotomy sample). Examples include but are not limited to delayed PET imaging, dynamic whole body PET imaging (GDA), organ or tissue-specific physiologic activity quantification (eg, glomerular filtration rate, quantitative pulmonary perfusion, among others).

## CONFLICTS OF INTEREST

None.

## REFERENCES

1. Cherry SR, Jones T, Karp JS, et al. Total-body PET: maximizing sensitivity to create new opportunities for clinical research and patient care. J Nucl Med 2018;59(1):3–12.
2. Badawi RD, Shi H, Hu P, et al. First human imaging studies with the EXPLORER total-body PET scanner. J Nucl Med 2019;60(3):299–303.
3. Alavi A, Werner TJ, Høilund-Carlsen PF. What can Be and what cannot Be accomplished with PET: rectifying ongoing Misconceptions. Clin Nucl Med 2017;42(8):603.
4. Alavi A, Newberg AB, Souder E, et al. Quantitative analysis of PET and MRI data in normal aging and Alzheimer's disease: atrophy weighted total brain metabolism and absolute whole brain metabolism as reliable discriminators. J Nucl Med 1993;34(10):1681–7.
5. Saboury B, Salavati A, Brothers A, et al. FDG PET/CT in Crohn's disease: correlation of quantitative FDG PET/CT parameters with clinical and endoscopic surrogate markers of disease activity. Eur J Nucl Med Mol Imaging 2014;41(4):605–14.
6. Basu S, Saboury B, Werner T, et al. Clinical utility of FDG–PET and PET/CT in non-malignant thoracic disorders. Mol Imaging Biol 2011;13(6):1051–60.
7. Abdulla S, Salavati A, Saboury B, et al. Quantitative assessment of global lung inflammation following radiation therapy using FDG PET/CT: a pilot study. Eur J Nucl Med Mol Imaging 2014;41(2):350–6.
8. Høilund-Carlsen PF, Edenbrandt L, Alavi A. Global disease score (GDS) is the name of the game! Eur J Nucl Med Mol Imaging 2019;46(9):1768–72.
9. Raynor WY, Al-Zaghal A, Zadeh MZ, et al. Metastatic seeding Attacks bone marrow, not bone: rectifying ongoing misconceptions. PET Clin 2019;14(1):135–44.
10. Raynor WY, Zadeh MZ, Kothekar E, et al. Evolving role of PET-based novel quantitative techniques in the management of hematological malignancies. PET Clin 2019;14(3):331–40.
11. Raynor WY, Jonnakuti VS, Zirakchian Zadeh M, et al. Comparison of methods of quantifying global synovial metabolic activity with FDG-PET/CT in rheumatoid arthritis. Int J Rheum Dis 2019;22(12):2191–8.
12. Khosravi M, Peter J, Wintering NA, et al. 18F-FDG is a superior indicator of cognitive performance compared to 18F-florbetapir in Alzheimer's disease and mild cognitive impairment evaluation: a global quantitative analysis. J Alzheimers Dis 2019;70(4):1197–207.
13. Saboury B, Parsons MA, Moghbel M, et al. Quantification of aging effects upon global knee inflammation by 18F-FDG-PET. Nucl Med Commun 2016;37(3):254–8.
14. Peter J, Houshmand S, Werner TJ, et al. Applications of global quantitative 18F-FDG-PET analysis in temporal lobe epilepsy. Nucl Med Commun 2015;1. https://doi.org/10.1097/mnm.0000000000000440.
15. Fardin S, Gholami S, Samimi S, et al. Global quantitative techniques for positron emission tomographic assessment of disease activity in cutaneous T-cell lymphoma and response to treatment. JAMA Dermatol 2016;152(1):103–5.
16. Marin-Oyaga VA, Salavati A, Houshmand S, et al. Feasibility and performance of an adaptive contrast-oriented FDG PET/CT quantification technique for global disease assessment of malignant pleural mesothelioma and a brief review of the literature. Hell J Nucl Med 2015;18(1):11–8.
17. Basu S, Zaidi H, Salavati A, et al. FDG PET/CT methodology for evaluation of treatment response in lymphoma: from "graded visual analysis" and "semiquantitative SUVmax" to global disease burden assessment. Eur J Nucl Med Mol Imaging 2014;41(11):2158–60.
18. Seraj SM, Ayubcha C, Zadeh MZ, et al. The evolving role of PET-based novel quantitative techniques in the interventional radiology procedures of the liver. PET Clin 2019;14(4):419–25.
19. Sherer Y, Shoenfeld Y. Mechanisms of disease: atherosclerosis in autoimmune diseases. Nat Clin Pract Rheumatol 2006;2(2):99–106.

20. Diani M, Altomare G, Reali E. T helper cell subsets in clinical manifestations of psoriasis. J Immunol Res 2016;2016:7692024.

21. Pinu FR, Beale DJ, Paten AM, et al. Systems biology and multi-omics integration: viewpoints from the metabolomics research community. Metabolites 2019; 9(4). https://doi.org/10.3390/metabo9040076.

22. Mardinoglu A, Boren J, Smith U, et al. Systems biology in hepatology: approaches and applications. Nat Rev Gastroenterol Hepatol 2018;15(6): 365–77.

23. Hanahan D, Weinberg RA. Hallmarks of cancer: the next generation. Cell 2011;144(5):646–74.

24. Basu S, Kwee TC, Gatenby R, et al. Evolving role of molecular imaging with PET in detecting and characterizing heterogeneity of cancer tissue at the primary and metastatic sites, a plausible explanation for failed attempts to cure malignant disorders. Eur J Nucl Med Mol Imaging 2011; 38(6):987–91.

25. Mankoff DA, Pantel AR, Viswanath V, et al. Advances in PET Diagnostics for guiding targeted cancer therapy and studying in vivo cancer biology. Curr Pathobiol Rep 2019;7(3):97–108.

26. Surti S, Pantel AR, Karp JS. Total Body PET: Why, How, What for? IEEE Transactions on Radiation and Plasma Medical Sciences 2020;4(3):283–92. Available at: https://ieeexplore.ieee.org/abstract/document/9056798/?casa_token=NTPSPgSONToAAAAA:zifFWCuiZyM0xSEYlo9QNC_EdO0iThLYJwMV_Scs5qtYpvcfPAFAGQy1tkPLTamVsaRjkqosAQ.

27. Pauwels EK, Ribeiro MJ, Stoot JH, et al. FDG accumulation and tumor biology. Nucl Med Biol 1998; 25(4):317–22.

28. Zhuang H, Pourdehnad M, Lambright ES, et al. Dual time point 18F-FDG PET imaging for differentiating malignant from inflammatory processes. J Nucl Med 2001;42(9):1412–7.

29. Basu S, Kung J, Houseni M, et al. Temporal profile of fluorodeoxyglucose uptake in malignant lesions and normal organs over extended time periods in patients with lung carcinoma: implications for its utilization in assessing malignant lesions. Q J Nucl Med Mol Imaging 2009;53(1):9.

30. Cheng G, Alavi A, Lim E, et al. Dynamic changes of FDG uptake and clearance in normal tissues. Mol Imaging Biol 2013;15(3):345–52.

31. Cherry SR, Badawi RD, Karp JS, et al. Total-body imaging: transforming the role of positron emission tomography. Sci Transl Med 2017;9(381). https://doi.org/10.1126/scitranslmed.aaf6169.

32. Hustinx R, Smith RJ, Benard F, et al. Dual time point fluorine-18 fluorodeoxyglucose positron emission tomography: a potential method to differentiate malignancy from inflammation and normal tissue in the head and neck. Eur J Nucl Med 1999;26(10): 1345–8.

33. Cheng G, Torigian DA, Zhuang H, et al. When should we recommend use of dual time-point and delayed time-point imaging techniques in FDG PET? Eur J Nucl Med Mol Imaging 2013;40(5):779–87.

34. Viswanath V, Daube-Witherspoon ME, Schmall JP, et al. Development of pet for total-body imaging. Acta Phys Pol B 2017;48(10):1555–66.

35. Ross JS, Stagliano NE, Donovan MJ, et al. Atherosclerosis and cancer: common molecular pathways of disease development and progression. Ann N Y Acad Sci 2001;947:271–92 [discussion: 292–3].

36. Ross JS, Stagliano NE, Donovan MJ, et al. Atherosclerosis: a cancer of the blood vessels? Pathol Patterns Rev 2001;116(suppl_1):S97–107.

37. Tapia-Vieyra JV, Delgado-Coello B, Mas-Oliva J. Atherosclerosis and cancer; A resemblance with far-reaching implications. Arch Med Res 2017; 48(1):12–26.

38. Ogawa A, Kanda T, Sugihara S, et al. Risk factors for myocardial infarction in cancer patients. J Med 1995;26(5–6):221–33.

39. Dardiotis E, Aloizou A-M, Markoula S, et al. Cancer-associated stroke: pathophysiology, detection and management. Int J Oncol 2019;54(3):779–96.

40. Yun M, Yeh D, Araujo LI, et al. F-18 FDG uptake in the large arteries. Clin Nucl Med 2001;26(4):314–9.

41. Beheshti M, Saboury B, Mehta NN, et al. Detection and global quantification of cardiovascular molecular calcification by fluoro18-fluoride positron emission tomography/computed tomography–a novel concept. Hell J Nucl Med 2011;14(2):114–20.

42. Moghbel M, Al-Zaghal A, Werner TJ, et al. The role of PET in evaluating atherosclerosis: a critical review. Semin Nucl Med 2018;48(6):488–97.

43. Høilund-Carlsen PF, Sturek M, Alavi A, et al. Atherosclerosis imaging with 18F-sodium fluoride PET: state-of-the-art review. Eur J Nucl Med Mol Imaging 2020;47(6):1538–51.

44. Schmall JP, Karp JS, Alavi A. The potential role of total body PET imaging in assessment of atherosclerosis. PET Clin 2019;14(2):245–50.

45. Sydow BD, Srinivas SM, Newberg A, et al. Deep venous thrombosis on F-18 FDG PET/CT imaging. Clin Nucl Med 2006;31(7):403–4.

46. Sharma P, Kumar R, Singh H, et al. Imaging thrombus in cancer patients with FDG PET–CT. Jpn J Radiol 2012;30(2):95–104.

47. Hess S, Madsen PH, Basu S, et al. Potential role of FDG PET/CT imaging for assessing venous thromboembolic disorders. Clin Nucl Med 2012;37(12):1170–2.

48. Bukhari A, Kesari V, Sirous R, et al. Increased cortical glycolysis following CD19 CART therapy: a radiographic surrogate for an altered blood-brain barrier. Blood 2019;134(Supplement_1):4454.

49. Holtzman NG, Bentzen SM, Kesari V, et al. Immune effector cell-associated neurotoxicity syndrome (ICANS) after CD19-directed chimeric antigen

receptor T-cell therapy (CAR-T) for large B-cell lymphoma: predictive biomarkers and clinical outcomes. Blood 2019;134(Supplement_1):3239.

50. Basu S, Kwee TC, Torigian D, et al. Suboptimal and inadequate quantification: an alarming crisis in medical applications of PET. Eur J Nucl Med Mol Imaging 2011;38(7):1381.

51. Lu HD, Wang LZ, Wilson BK, et al. Copper loading of preformed nanoparticles for PET-imaging applications. ACS Appl Mater Interfaces 2018;10(4): 3191–9.

52. Blake GM, Siddique M, Frost ML, et al. Imaging of site specific bone turnover in osteoporosis using positron emission tomography. Curr Osteoporos Rep 2014;12(4):475–85.

53. Raijmakers P, Temmerman OPP, Saridin CP, et al. Quantification of F-18-Fluoride kinetics: evaluation of simplified methods. J Nucl Med 2014;55(7): 1122–7.

54. Al-beyatti Y, Siddique M, Frost ML, et al. Precision of F-18-fluoride PET skeletal kinetic studies in the assessment of bone metabolism. Osteoporos Int 2012;23(10):2535–41.

55. Rankin LC, Artis D. Beyond host defense: emerging functions of the immune system in regulating complex tissue physiology. Cell 2018;173(3):554–67.

56. Wibmer AG, Hricak H, Ulaner GA, et al. Trends in oncologic hybrid imaging. Eur J Hybrid Imaging 2018;2(1):1.

57. Chen DL. Promising advances for imaging lung macrophage recruitment. Am J Respir Crit Care Med 2020;201(1):11–3.

58. Mao L, Jin H, Wang M, et al. Neurologic manifestations of hospitalized patients with coronavirus disease 2019 in Wuhan, China. JAMA Neurol 2020. https://doi.org/10.1001/jamaneurol.2020.1127.

59. Carod-Artal FJ. Neurological complications of coronavirus and COVID-19. Rev Neurol 2020;70(9): 311–22.

60. Henrich TJ, Hsue PY, VanBrocklin H. Seeing is believing: nuclear imaging of HIV persistence. Front Immunol 2019;10:2077. Available at: https://apps. webofknowledge.com//full_record.do?product=W OS&search_mode=CitingArticles&qid=27&SID= 7EqLigFTSJIT32iWyNA&page=3&doc=22.

61. Lloyd-Jones D, Adams R, Carnethon M, et al. Heart disease and stroke statistics–2009 update: a report from the American Heart Association Statistics Committee and stroke statistics subcommittee. Circulation 2009;119(3):480–6.

62. Lozano R, Naghavi M, Foreman K, et al. Global and regional mortality from 235 causes of death for 20 age groups in 1990 and 2010: a systematic analysis for the Global Burden of Disease Study 2010. Lancet 2012;380(9859):2095–128.

63. Wilms G, Baert AL. The history of angiography. J Belge Radiol 1995;78(5):299–302.

64. Agatston AS, Janowitz WR, Hildner FJ, et al. Quantification of coronary artery calcium using ultrafast computed tomography. J Am Coll Cardiol 1990; 15(4):827–32.

65. Willemink MJ, van der Werf NR, Nieman K, et al. Coronary artery calcium: a technical argument for a new scoring method. J Cardiovasc Comput Tomogr 2019;13(6):347–52.

66. Alavi A, Werner TJ, Høilund-Carlsen PF. PET-based imaging to detect and characterize cardiovascular disorders: unavoidable path for the foreseeable future. J Nucl Cardiol 2018;25(1):203–7.

67. Alavi A, Werner TJ, Høilund-Carlsen PF. What can be and what cannot be accomplished with PET to detect and characterize atherosclerotic plaques. J Nucl Cardiol 2018;25(6):2012–5.

68. McKenney-Drake ML, Moghbel MC, Paydary K, et al. 18F-NaF and 18F-FDG as molecular probes in the evaluation of atherosclerosis. Eur J Nucl Med Mol Imaging 2018;45(12):2190–200.

69. Raynor WY, Borja AJ, Rojulpote C, et al. 18F-sodium fluoride: an emerging tracer to assess active vascular microcalcification. J Nucl Cardiol 2020. https://doi.org/10.1007/s12350-020-02138-9.

70. Blomberg BA, Thomassen A, Takx RAP, et al. Delayed 18F-fluorodeoxyglucose PET/CT imaging improves quantitation of atherosclerotic plaque inflammation: results from the CAMONA study. J Nucl Cardiol 2014;21(3):588–97.

71. Blomberg BA, Thomassen A, Takx RAP, et al. Delayed sodium 18F-fluoride PET/CT imaging does not improve quantification of vascular calcification metabolism: results from the CAMONA study. J Nucl Cardiol 2014;21(2):293–304.

72. Kwiecinski J, Berman DS, Lee S-E, et al. Three-hour delayed imaging improves assessment of coronary 18F-sodium fluoride PET. J Nucl Med 2019;60(4): 530–5.

73. Zhuang H, Alavi A. Evolving role of PET in pediatric disorders. PET Clin 2020;15(3):xv–xvii.

74. Viale PH. The American Cancer Society's facts & figures: 2020 edition. J Adv Pract Oncol 2020;11. https://doi.org/10.6004/jadpro.2020.11.2.1.

75. Waeber G. Just listen to your patient, he is telling you the diagnosis. In: Forum Médical Suisse. Vol 19. EMH Media; 2019:373-373.